

## **Cloud Optical Properties from the Multifilter Shadowband Radiometer (MFRSRCLDOD): An ARM Value-Added Product**

DD Turner  
Q Min  
K Gaustad

C Lo  
D Zhang

July 2021



## **DISCLAIMER**

This report was prepared as an account of work sponsored by the U.S. Government. Neither the United States nor any agency thereof, nor any of their employees, makes any warranty, express or implied, or assumes any legal liability or responsibility for the accuracy, completeness, or usefulness of any information, apparatus, product, or process disclosed, or represents that its use would not infringe privately owned rights. Reference herein to any specific commercial product, process, or service by trade name, trademark, manufacturer, or otherwise, does not necessarily constitute or imply its endorsement, recommendation, or favoring by the U.S. Government or any agency thereof. The views and opinions of authors expressed herein do not necessarily state or reflect those of the U.S. Government or any agency thereof.

# **Cloud Optical Properties from the Multifilter Shadowband Radiometer (MFRSRCLDOD): An ARM Value-Added Product**

DD Turner, National Oceanic and Atmospheric Administration  
C Lo, Pacific Northwest National Laboratory (PNNL)  
Q Min, State University of New York, Albany  
D Zhang, PNNL  
K Gaustad, PNNL

July 2021

Work supported by the U.S. Department of Energy,  
Office of Science, Office of Biological and Environmental Research

## Acronyms and Abbreviations

ARM	Atmospheric Radiation Measurement
ARSCL	Active Remote Sensing of Clouds
FSSP	forward-scattering spectrometer probe
GOES	Geostationary Operational Environmental Satellite
IRT	infrared thermometer
LWP	liquid water path
MFRSR	multifilter rotating shadowband radiometer
MFRSRCLDOD	Cloud Optical Properties from the Multifilter Shadowband Radiometer
MWR	microwave radiometer
NetCDF	Network Common Data Form
PWV	precipitable water vapor
SGP	Southern Great Plains
UTC	Coordinated Universal Time
VAP	value-added product

## Contents

Acronyms and Abbreviations .....	iii
1.0 Introduction .....	1
2.0 Input Data .....	1
3.0 Output Data .....	3
4.0 Algorithm/Method .....	3
5.0 Examples .....	6
6.0 Known Caveats.....	9
7.0 References .....	9
Appendix A – Input Data .....	A.1
Appendix B – Output Variables.....	B.1

## Figures

1 $I_0$ calibration quicklook plot .....	4
2 Distribution of the uncertainties in cloud optical depth for uncertainties in A) $I$ , B) $I_0$ , C) LWP, D) surface albedo. Panel E shows the distribution of the total uncertainty in the cloud optical depth for this 6-month period (January-June 2003). .....	6
3 Distribution of the uncertainties in effective radius for uncertainties in I, B) $I_0$ , C) LWP, D) surface albedo. Panel E shows the distribution of the total uncertainty in the cloud optical depth for this 6-month period (January-June 2003). .....	6
4 Quicklook image showing the cloud optical properties for March 11, 2003. ....	7
5 Retrieved cloud optical properties for 6 months of data starting 1 Jan 2003. A) retrieved $\tau$ , B) retrieved $r_e$ , C) cloud fraction from shortwave flux analysis VAP, D) cloud base height from ARSCL VAP, E) LWP from the MWR. ....	8
6 Distributions of the retrieved cloud optical depth (A) and effective radius (B) from 1 January to 30 June 2003. Panel C, D, and E show the corresponding cloud fraction, cloud height and LWP.....	8

## Tables

1 Input variables. ....	A.1
2 Output variables. ....	B.1

## 1.0 Introduction

The microphysical properties of clouds play an important role in studies of global climate change. Observations from satellites and surface-based systems have been used to infer cloud optical depth and effective radius. Min and Harrison (1996) developed an inversion method to infer the optical depth of liquid water clouds from narrow-band spectral multifilter rotating shadowband radiometer (MFRSR) measurements (Harrison et al. 1994). Their retrieval also uses the total liquid water path (LWP) measured by a microwave radiometer (MWR) to obtain the effective radius of the warm cloud droplets. Their results were compared with Geostationary Operational Environmental Satellite (GOES) retrieved values at the Atmospheric Radiation Measurement (ARM) Southern Great Plains (SGP) observatory (Min and Harrison 1996). Min et al. (2003) also validated the retrieved cloud optical properties against in situ observations, showing that the retrieved cloud effective radius agreed well with the in situ forward-scattering spectrometer probe (FSSP) observations. The retrieved cloud optical properties from Min et al. (2003) were used also as inputs to an atmospheric shortwave model, and the computed fluxes were compared with surface pyranometer observations.

The Min and Harrison algorithm has been incorporated into an ARM value-added product (VAP) called Cloud Optical Properties from the Multifilter Shadowband Radiometer (MFRSRCLDOD). This version of the VAP (1 min) uses the diffuse transmission at 415 nm from the MFRSR. Therefore, the results are only valid for “horizontally homogeneous” stratiform clouds with optical depths larger than approximately 7. The retrieval assumes a single cloud layer consisting solely of liquid water drops. As specified by Min and Harrison (1996), the wavelength at 415 nm was chosen due to the lack of gaseous absorption and the relatively constant surface albedo (in the absence of snow) at this wavelength.

The MFRSRCLDOD VAP (henceforth referred to as “the VAP”) retrieves cloud optical depth ( $\tau$ ) from the MFRSR measurements. If the LWP is available from a coincident MWR observation, then the droplet effective radius ( $r_e$ ) can be determined. Knowledge of the estimated  $r_e$  can be used to improve the estimate of  $\tau$  because there is a slight dependence on the extinction coefficient, single scattering albedo, and asymmetry parameter on effective radius at this wavelength. However, if the MWR’s LWP is not available, then the VAP assumes that  $r_e = 8.0 \mu\text{m}$ . The primary output from the VAP is  $\tau$  and  $r_e$ .

The VAP also provides 1-sigma uncertainties for  $\tau$  and  $r_e$  by propagating the uncertainties in the top-of-atmosphere irradiance ( $I_0$ ), the measured irradiance ( $I$ ), the MWR’s LWP, and the surface albedo.

## 2.0 Input Data

The input files for this VAP are standard ARM NetCDF products. To run this VAP properly, we need the following input files and data:<sup>1</sup>

---

<sup>1</sup> For details of the input variables, see Appendix A.

**Multifilter rotating shadowband radiometer instrument:**

mfrsr.b1/mfrsr7nch.b1

datastreams provide the observed irradiance data (I) from the MFRSR. This is a required input. The MFRSR was recently upgraded to replace its broadband measurement with a 1625-nm sensor. The MFRSRCLDOD VAP can take the upgraded 7-channel MFRSR measurements as inputs.

**Microwave radiometer instruments:**

mwrret1liljclou.c2/mwrret1liljclou.c1/mwrret2turn.c1/mwrlos.b1

datastreams provide LWP, precipitable water vapor (PWV), and brightness temperatures from the MWR. This is an optional input. The VAP prefers to use mwrret1liljclou.c2 data to retrieve effective radius. If mwrret1liljclou.c2 is not available, the VAP takes mwrret1liljclou.c1, and then mwrret2turn.c1, and then mwrlos.b1. If available, the “be\_lwp” variable from MWRRET is used. If this variable is bad/missing, then “phys\_lwp” is used if good or indeterminate. If it is not available, then “stat2\_lwp” is used if good or indeterminate. If all are missing/bad, then the default effective radius = 8.0 um is used.

**Langley Value-Added Product:**

mfrsreal.c1/mfrsrlangley.c1/mfrsr7nchlangley.c1

datastreams provide the top-of-atmosphere irradiance ( $I_0$ ) data. This is a required input. For sites that are often cloudy, it is challenging to get mfrsrlangley.c1. We use manually produced Langley data (mfrsreal.c1) as inputs. The VAP will scan whether mfrsreal.c1 data are available. If the correspondent mfrsreal.c1 data are found, the VAP will prefer to use mfrsreal.c1.

**Shortwave Flux Value-Added Product:**

radflux1long.c2/radflux1long.c1

datastreams provide data for feature analyses regarding the cloud sky cover fraction. Cloud cover fraction is a required input for MFRSRCLDOD. The VAP looks for cloud cover fraction from Shortwave Flux Value-Added Products, or the Surface Spectral Albedo Value-Added Product, or the total sky imager instrument measurements.

**Cloud Base Height Value-Added Product:**

arslbn1cloth.c1/arsclkazrbnd1kollias.c1/arsclwacrbnd1kollias.c1

datastreams provide ancillary data for feature analyses regarding the height (and by inference the phase) of the clouds. This is an optional input.

**Infrared thermometer instrument:**

irt.b1/skyrad60.b1/mwrlos.b1

datastreams provide sky infrared temperature. This is an optional input.

**Surface Spectral Albedo Value-Added Product:**

surfspectralb1mlawer.c1

datastream provides fractional cloud cover.

**Total sky imager instrument:**

tskiskycover.b1/

datastream provide sky cover measurements.

### 3.0 Output Data

The name of the output file is:

sssMFRSRCIdOD1MinE13.C1.YYYYMMDD.hhmmss – 20 s data

Where:

SSS	the site of the instrument
MFRSR	the main instrument name
CIdOD1Min	identifies that this is Min’s version 1 VAP
E13	facility
YYYY	year, MM - month of the year, DD - day of the month, hh - hour of the day, mm - minute of the hour, ss - second of the minute of data start.

The detailed variable descriptions are in Table 2, Appendix B.

This VAP generates two quicklook plots: one is the  $I_0$  calibration in Figure 1 and the second is the cloud optical properties in Figure 4. The names of the quicklook files are:

YYYYMMDD\_quicklook.png  
Io\_YYYYMMDD\_quicklook.png

### 4.0 Algorithm/Method

The functioning heart of this VAP is the Nonlinear Least Squares retrieval algorithm of Min and Harrison (1996). This algorithm uses a parameterization of the scattering properties at 415 nm on the effective radius and LWP using Mie theory. The algorithm uses an adjoint formulation of the radiative transfer to maintain accuracy and improve its execution speed. It uses an iterative approach to retrieve both cloud optical depth and effective radius if an estimate of LWP is provided; otherwise the effective radius is assumed and the algorithm returns only optical depth.

The algorithm requires the atmospheric transmittance at 415 nm. This is easily computed using the observed irradiance  $I$  and the top of the atmosphere irradiance  $I_0$ , where  $I_0$  is computed from Langley



regressions on clear days. Because data from the MFRSR are used to obtain both  $I$  and  $I_0$ , the absolute calibration of the instrument is not required to get accurate observations of the atmospheric transmittance.

A previously developed VAP routinely analyzed the MFRSR data and computes  $I_0$ . However, the most accurate values of  $I_0$  are obtained only on days that are free of clouds and stable. Furthermore, a maximum of two Langley regressions could be computed for a single day. Because this VAP is concerned with cloud properties, the  $I_0$  values used are computed from  $I_0$  values determined on nearby clear-sky days. We have automated a procedure to determine an accurate value of  $I_0$ . The VAP reads in all of the  $I_0$  data that were determined to be good by the Langley analysis VAP for 3 months before and after the day currently being processed. From this large data set, we select the 20 closest in time  $I_0$  values. We then follow the procedure outlined in Michalsky et al. (2001) to select the best 10 of the 20 points; the mean value of these 10 points is used as the  $I_0$  for the processing. The uncertainty in  $I_0$  represented by the standard deviation about the mean  $I_0$  value of the 10 points is propagated to provide uncertainties in the retrieved cloud properties. Figure 1 shows a quicklook plot that displays all of the  $I_0$  values determined by the Langley algorithm VAP, the 20 closest points, and the mean and standard deviation of the  $I_0$  value used in the VAP.

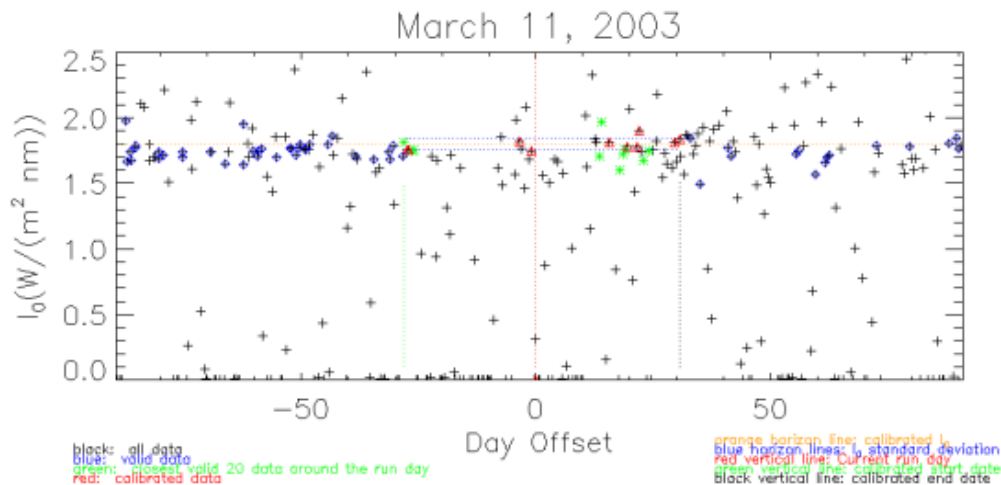


**Figure 1.**  $I_0$  calibration quicklook plot. See text for details.

The LWP from the MWR, while not critical for the execution of the VAP, does permit the retrieval of effective radius. The VAP applies some simple quality control to ensure that the reported LWP is valid. If the observed brightness temperature at either MWR frequency is below the cosmic background or above 100 K (the latter condition is usually indicative of rain), then the LWP value from the MWR is not used in the retrieval. Furthermore, because the uncertainty in the MWR's retrieval LWP is approximately 20 g m<sup>2</sup> (Westwater et al. 2001), the VAP does not use the MWR's observed LWP in the retrieval if the LWP is below this threshold. When no LWP is available, the retrieval algorithm assumes that the effective radius is 8  $\mu$ m.

The temporal resolution of the MFRSR irradiance data is 20 s, and therefore the ancillary inputs are interpolated to this time. The interpolation of the LWP is usually required. The LWP is interpolated across gaps of a maximum of 5 min. If the temporal gap is larger than this, then the retrieval is run without LWP input for those MFRSR samples.

Because this VAP can be run at sites that have a MFRSR, such as the ARM extended facilities, the VAP uses the retrieved optical depth and assumed effective radius to provide an estimate of the LWP using

$$\text{LWP} = (2/3) * \rho * \tau * r_e$$

Where  $\rho$  is the density of liquid water,  $\tau$  is retrieved by the VAP, and  $r_e$  was assumed. This provides estimates of the LWP at sites where MWRs are not deployed. However, due to the natural variability in  $r_e$  the uncertainty in this derived LWP is large. A flag is set in the output file to indicate if the output LWP is from the MWR or this calculation.

The retrieval algorithm operates at two temporal resolutions. It provides “instantaneous” retrievals at the nominal 20-s resolution of the MFRSR and “average” retrievals where the data have been averaged for 5 min centered upon the output sample time. The average retrievals are less sensitive to the spatial inhomogeneities in the cloud, which affect the diffuse irradiance field.

As indicated above, the VAP provides 1-sigma uncertainties for both the retrieved optical depth and effective radius by propagating the uncertainties in the input and assumed parameters. The uncertainty in the  $I_0$  value is the standard deviation about the mean  $I_0$  as described above. If the LWP is available from the MWR, the uncertainty in the LWP is assumed to be  $20 \text{ g m}^{-2}$ . The uncertainty in the observed irradiance is assumed to be 1%. The surface albedo, which is taken to be 0.036 at 415 nm in non-snow covered conditions, is assumed to have an uncertainty of  $\pm 0.01$ . These uncertainties are propagated individually using finite differences and combined as the root sum of squared errors (i.e., these uncertainties are assumed to be independent). The uncertainty in the retrieved optical depth is dominated by the uncertainty in  $I_0$ , while the uncertainty in the LWP is the dominant term in the effective radius uncertainty. Figures 2 and 3 present examples of distributions of each component of the total uncertainty to the uncertainty in  $\tau$  and  $r_e$ , respectively, as well as the distributions of the total uncertainty in each retrieved variable for data from the SGP site over a 6-month period.

Finally, this VAP provides some ancillary data to help the analyst find cases where the retrieval is valid. The fractional sky cover from the shortwave analysis VAP (Long and Gaustad 2004) is included because the retrievals from this VAP are only valid in overcast scenes. The cloud base height from the Active Remote Sensing of Clouds (ARSCL) VAP (Clothiaux et al. 2001), along with the infrared thermometer (IRT) sky brightness temperature, are included because the retrievals are also only valid for single-layer liquid water clouds. Therefore, the user should use these fields to help select the proper cases to analyze.

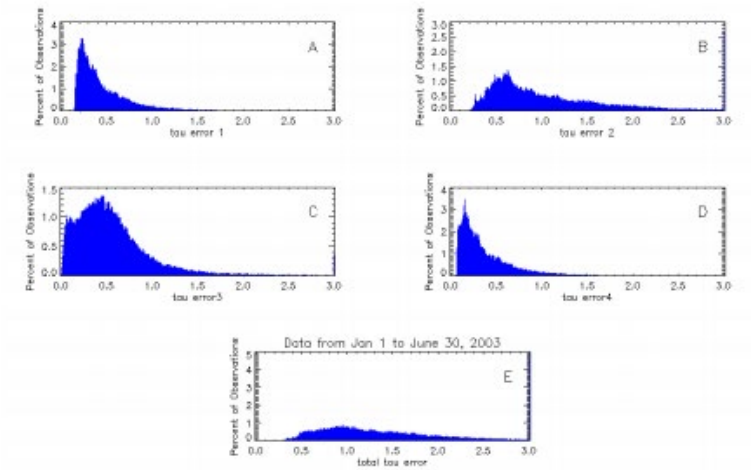


**Figure 2.** Distribution of the uncertainties in cloud optical depth for uncertainties in A) I, B)  $I_0$ , C) LWP, D) surface albedo. Panel E shows the distribution of the total uncertainty in the cloud optical depth for this 6-month period (January-June 2003).

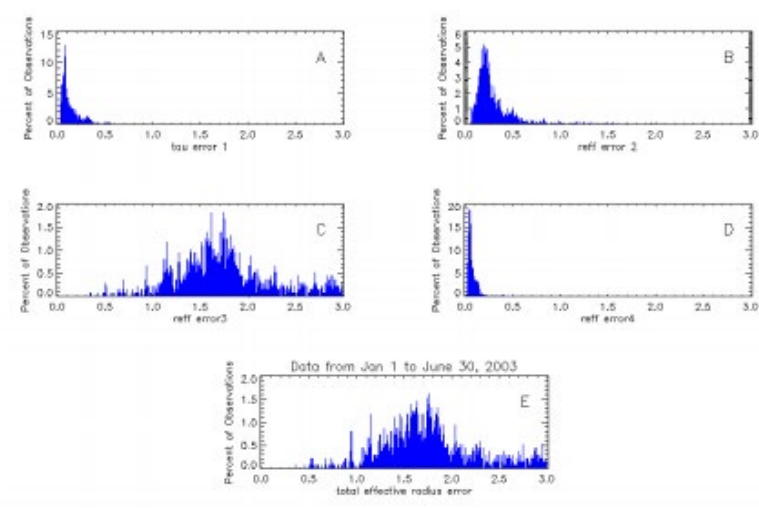


**Figure 3.** Distribution of the uncertainties in effective radius for uncertainties in A) I, B)  $I_0$ , C) LWP, D) surface albedo. Panel E shows the distribution of the total uncertainty in the cloud optical depth for this 6-month period (January-June 2003).

## 5.0 Examples

This VAP runs daily. Two quicklook plots are generated every day: one is the  $I_0$  calibration in Figure 1 as explained before and the other one is a five-panel plot for the cloud properties. Figure 4 gives an example for March 11, 2003. The data start around 13:50 Coordinated Universal Time (UTC) and end around 24:00. An overcast liquid water cloud persisted on this day, as the clouds were of low height and the effective radius was small, indicating the presence of small cloud drops. The first panel shows the derived cloud optical depth data for instantaneous (20-s) and averaged (5-min) resolutions. The second panel shows the retrieved effective radius. The third panel shows the ratios of the total uncertainty to the

retrieved data. Panel four displays the cloud fraction and cloud height. The last panel shows the LWP from MWR or the LWP from the default effective radius (which it does not have on this day, because all of the MWR LWP data were valid).

The six months of data from January 1 to June 30, 2003 are shown in Figure 5 and the distributions of the cloud properties for this period are shown in Figure 6. Only valid data meeting the following criteria are included in Figures 5 and 6. The criteria are cloud fraction > 90 %, infrared temperature > 268 (- 50°C), cloud base height < 4 km, optical depth > 7, effective radius  $\neq 8.00 \mu\text{m}$  (because an effective radius equal to  $8 \mu\text{m}$  implies that the LWP from the MWR was not available or not used), and effective radius > 0.

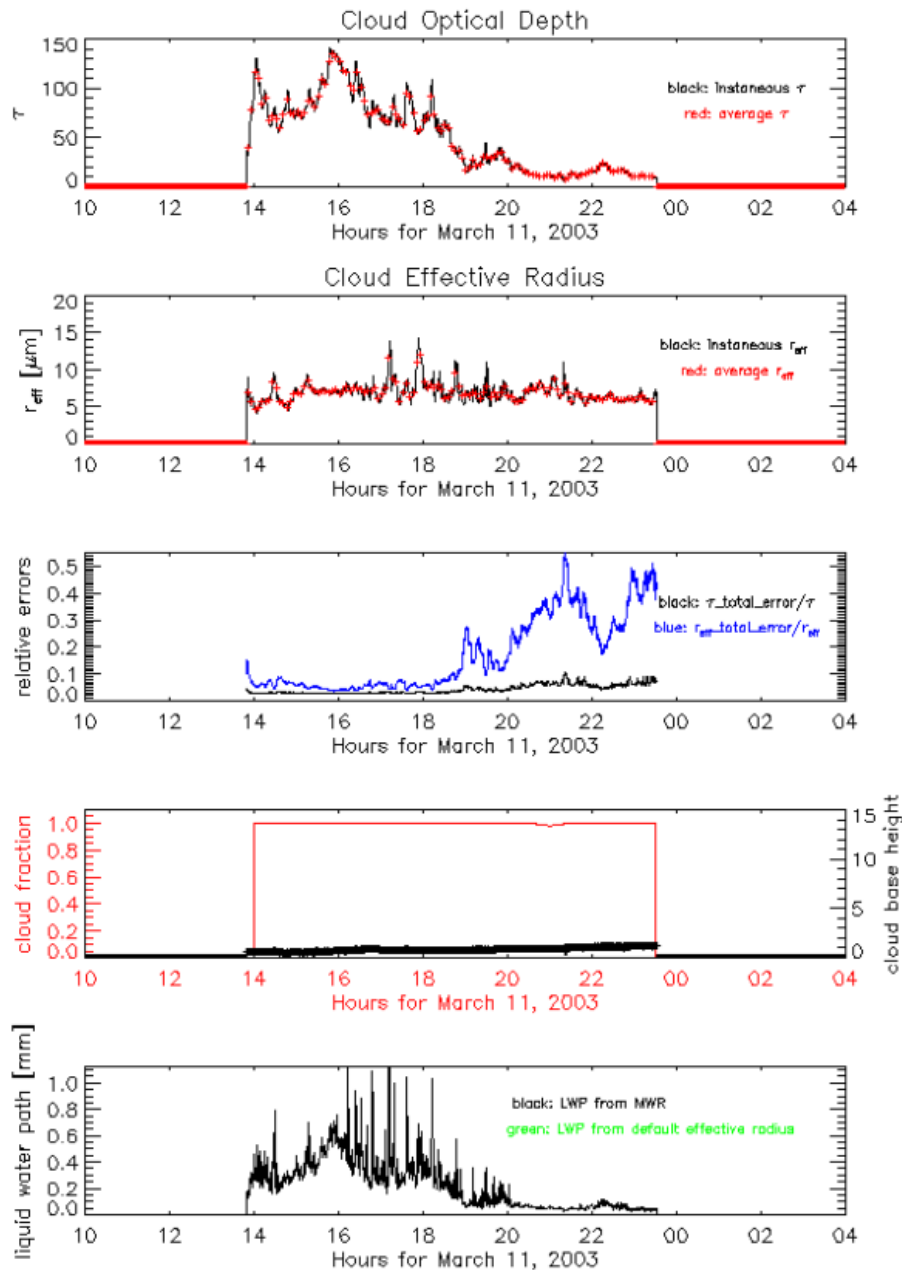


**Figure 4.** Quicklook image showing the cloud optical properties for March 11, 2003.

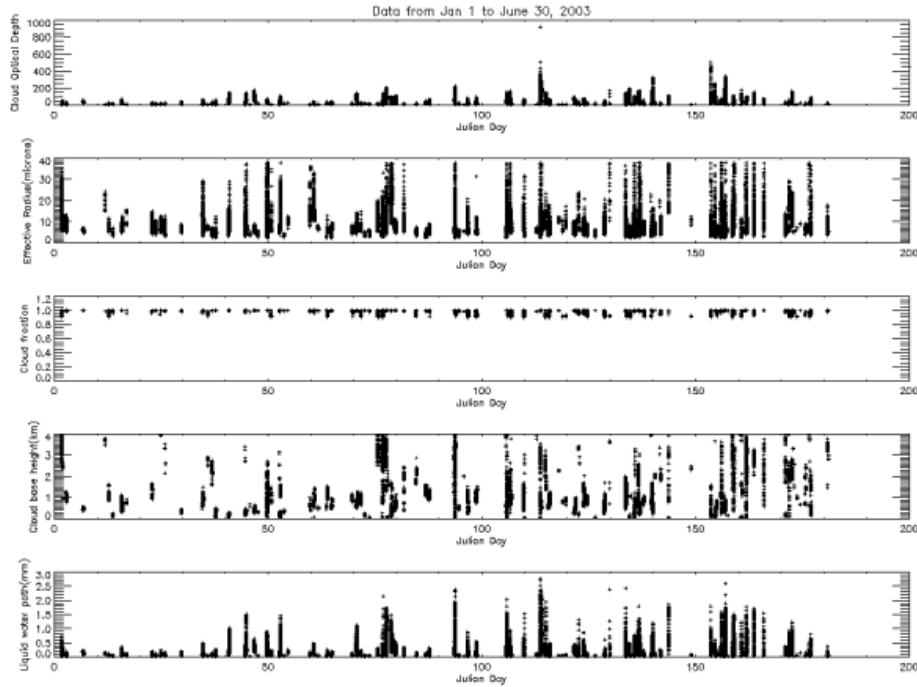


**Figure 5.** Retrieved cloud optical properties for 6 months of data starting 1 January 2003. A) retrieved  $\tau$ , B) retrieved  $r_e$ , C) cloud fraction from shortwave flux analysis VAP, D) cloud base height from ARSCL VAP, E) LWP from the MWR.

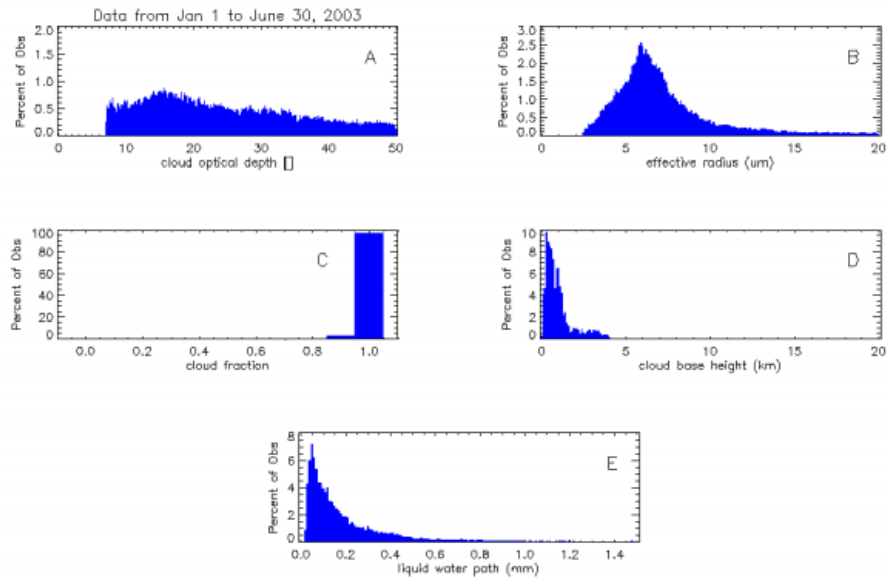


**Figure 6.** Distributions of the retrieved cloud optical depth (A) and effective radius (B) from 1 January to 30 June 2003. Panel C, D, and E show the corresponding cloud fraction, cloud height, and LWP.

## 6.0 Known Caveats

- Only valid for overcast conditions where cloud is liquid. Because there is no gaseous absorption at this wavelength (415 nm), the retrieval will be valid for both single-layer and multiple-layer cloud conditions, as long as all layers are overcast and composed entirely of liquid drops.
- Assumes the surface is not covered with snow or ice.
- Biases in the MWR's LWP, especially for small optical depths, will bias the retrieved effective radius.

## 7.0 References

Clothiaux, EE, MA Miller, RC Perez, DD Turner, KP Moran, BE Martner, TP Ackerman, GG Mace, RT Marchand, KB Widener, DJ Rodriguez, T Uttal, JH Mather, CJ Flynn, KL Gaustad, and B Ermold. 2001. The ARM millimeter wave cloud radars (MMCRs) and the active remote sensing of clouds (ARSCL) Value Added Product (VAP). U.S. Department of Energy. [ARM VAP-002-1](#).

Harrison, LC, JJ Michalsky, and J Berndt. 1994. "Automated multi-filter rotating shadowband radiometer: an instrument for optical depth and radiation measurements." *Applied Optics* 33(22): 5118–5125, <https://doi.org/10.1364/AO.33.005118>

Long, CN, and KL Gaustad. 2004. The shortwave (SW) clear-sky detection and fitting algorithm: algorithm operational details and explanations. Revision 1. U.S. Department of Energy. [DOE/SC-ARM-TR-004-1](#).

Michalsky, JJ, JA Schlemmer, WE Berkheiser, JL Berndt, LC Harrison, NS Laulainen, NR Larson, and JC Barnard. 2001. "Multiyear measurements of aerosol optical depth in the Atmospheric Radiation Measurement and Quantitative Links programs." *Journal of Geophysical Research – Atmospheres* 106(D11): 12099–12107, <https://doi.org/10.1029/2001JD900096>

Min, Q, and LC Harrison. 1996. "Cloud properties derived from surface MFRSR measurements and comparison with GOES results at the ARM SGP site." *Geophysical Research Letters* 23(13):1641–1644, <https://doi.org/10.1029/96GL01488>

Min, Q, M Duan, and R Marchand. 2003. "Validation of surface retrieved cloud optical properties with in situ measurements at the Atmospheric Radiation Measurement Program (ARM) South Great Plains site." *Journal of Geophysical Research – Atmospheres* 108(D17): 4547, <https://doi.org/10.1029/2003JD003385>

Westwater, ER, Y Han, MD Shupe, and SY Matrosov. 2001. "Analysis of integrated cloud liquid and precipitable water vapor retrievals from MWRs during SHEBA." *Journal of Geophysical Research – Atmospheres* 106(D23): 32,019-32,030.

## Appendix A

### Input Data

Table 1 lists the various ARM datastreams used in the VAP for data, along with the specific variables in files that are used in processing.

**Table 1.** Input variables.

Variable Retrieved	Possible Data Sources	Name in Source
Cloud Base Height Best Estimate	arsclbnd1cloth.c1 arsclwacrbnd1kollias.c1 arsclkazrbnd1kollias.c1	CloudBaseBestEstimate cloud_base_best_estimate
Sky/cloud infrared temperature	irt.b1 skyrad60s.b1 mwrlos.b1	sky_ir_temp sky_ir_temp
TOA direct normal irradiance corrected for earth-sun distance from robustly filtered Langley regressions for filter <1, 2, 3, 4, 5>	mfrsrca1.c1 mfrsrlangley.c1 mfrsr7nchlangley.c1	Io_filter<1, 2, 3, 4, 5> barnard_solar_constant_sdist_filter<1, 2, 3, 4, 5> barnard_solar_constant_sdist_filter<1, 2, 3, 4, 5>
Cosine solar zenith angle	mfrsr.b1 mfrsr7nch.b1	cosine_solar_zenith_angle
Narrowband direct normal irradiance, filter <1, 2, 3, 4, 5>, cosine corrected	mfrsr.b1 mfrsr7nch.b1	direct_normal_narrowband_filter<1, 2, 3, 4, 5> direct_normal_narrowband_filter<1, 2, 3, 4, 5>
Narrowband hemispheric irradiance, filter <1, 2, 3, 4, 5>, offset and cosine corrected	mfrsr.b1 mfrsr7nch.b1	hemisp_narrowband_filter<1, 2, 3, 4, 5>
Nominal calibration factor using standard lamp, applied to filter1 data	mfrsr.b1 mfrsr7nch.b1	nominal_calibration_factor_filter<1, 2, 3, 4, 5>

Variable Retrieved	Possible Data Sources	Name in Source
Liquid water path best-estimate value	mwrret1liljclou.c2 mwrret1liljclou.c1 mwrret2turn.c1 mwrlos.b1	be_lwp be_lwp phys_lwp liq
Precipitable water vapor best-estimate value	mwrret1liljclou.c2 mwrret1liljclou.c1 mwrret2turn.c1 mwrlos.b1	be_lwp be_lwp phys_lwp liq
Frequency Sky brightness temperature at 23.8 GHz	mwrret2turn.c1  mwrret1liljclou.c2 mwrret1liljclou.c1 mwrret2turn.c1 mwrlos.b1	freq  tbsky23 tbsky23  tbsky23
Sky brightness temperature at 31.4 GHz	mwrret1liljclou.c2 mwrret1liljclou.c1 mwrret2turn.c1 mwrlos.b1	tbsky31 tbsky31 tbsky31 tbsky31
Instantaneous observed brightness temperature	mwrret2turn.c1	tbsky_obs
Precipitable water vapor retrieved using a physical/iterative approach	mwrret1liljclou.c2 mwrret1liljclou.c1 mwrret2turn.c1	phys_lwp phys_lwp phys_lwp
Cloud liquid water path retrieved using predicted mean radiating temperatures and retrieval coefficients	mwrret1liljclou.c2 mwrret1liljclou.c1 mwrret2tirm/c1	stat2_lwp stat2_lwp stat2_lwp
Estimated shortwave fractional sky cover	radflux1long.c2 radflux1long.c1 15swfanalsirs1long.c1	cloudfraction_shortwave  cloudfraction
Best estimate Narrowband surface albedo at the 10m tower	surfspecalb1mlawer.c1	be_surface_albedo_mfr_narrowband_10m
Percent opaque cloud	tsiskycover.b1	Percent_opaque
Percent thin cloud	tsiskycover.b1	Percent_thin



## Appendix B

### Output Variables

Table 2 lists the detailed descriptions of the variables for the MFRSRCLDOD1MIN VAP output file. Primary variables are noted in bold.

**Table 2. Output variables.**

Variable Name	Long Name	Units
time_offset	Time offset from base_time	<Set at Runtime>
Base_time	Base time in Epoch	Seconds since 1970-1-1 0:00:00 0:00
time	Time offset from midnight	<Set at Runtime>
qc_time	Quality check results on field: Time offset from midnight	unitless
<b>optical_depth_instantaneous</b>	Cloud Optical Depth (instantaneous)	unitless
qc_optical_depth_instantaneous	Quality check results on field: Cloud Optical Depth (Instantaneous)	unitless
effective_radius_instantaneous	Effective Radius (Instantaneous)	microns
qc_effective_radius_instantaneous	Quality check results of field: Effective Radius (Instantaneous)	unitless
optical_depth_average	Five-Minute Running Average of Cloud Optical Depth	unitless
qc_optical_depth_average	Quality check results on field: Five-Minute Running Average of Cloud Optical Depth	unitless
effective_radius_average	Five-Minute Running Average of Effective Radius	microns
qc_effective_radius_average	Quality check results on field: Five-Minute Running Average of Effective Radius	unitless
cldtaui_error1	Cloud Tau Error1 (1% uncertainty in total irradiance)	unitless
qc_cldtaui_error1	Quality check results on field: Cloud Tau Error1 (1% uncertainty in total irradiance)	unitless
cldtaui_error2	Cloud Tau Error2 (uncertainty is standard deviation of calibrated 10 Inought points)	unitless
qc_cldtaui_error2	Quality check results on field: Cloud Tau Error2 (uncertainty is standard deviation of calibrated 10 Inought points)	unitless
cldtaui_error3	Cloud Tau Error3 (uncertainty in liquid water path (lwp) 0.001mm larger, using scaling factor with 0.015 mm)	unitless

Variable Name	Long Name	Units
qc_cldtaui_error3	Quality check results on field: Cloud Tau Error3 (uncertainty in liquid water path (lwp) 0.001mm larger, using scaling factor with 0.015 mm)	unitless
cldtaui_error4	Cloud Tau Error4 (uncertainty is 0.01 in surface albedo)	unitless
qc_cldtaui_error4	Quality check results on field: Cloud Tau Error4 (uncertainty is 0.01 in surface albedo)	unitless
cldtaui_error5	Cloud Tau Error5 (uncertainty in 3um higher of effective radius when there is no MWR data)	unitless
qc_cldtaui_error5	Quality check results on field: Cloud Tau Error5 (uncertainty in 3um higher of effective radius when there is no MWR data)	unitless
cldtaui_toterror	Instantaneous Cloud Tau Total Uncertainty	unitless
qc_cldtaui_toterror	Quality check results on field: Instantaneous Cloud Tau Total Uncertainty	unitless
cldtaua_error1	Cloud Tauga Error1 (1% uncertainty in total irradiance)	unitless
qc_cldtaua_error1	Quality check results on field: Cloud Tauga Error1 (1% uncertainty in total irradiance)	unitless
cldtaua_error2	Cloud Tauga Error2 (uncertainty is standard deviation of calibrated 10 Inought points)	unitless
qc_cldtaua_error2	Quality check results on field: Cloud Tauga Error2 (uncertainty is standard deviation of calibrated 10 Inought points)	unitless
cldtaua_error3	Cloud Tauga Error3 (uncertainty in liquid water path (lwp) 0.001mm larger, using scaling factor with 0.015 mm)	unitless
qc_cldtaua_error3	Quality check results on field: Cloud Tauga Error3 (uncertainty in liquid water path (lwp) 0.001mm larger, using scaling factor with 0.015 mm)	unitless
cldtaua_error4	Cloud Tauga Error4 (uncertainty is 0.01 in surface albedo)	unitless
qc_cldtaua_error4	Quality check results on field: Cloud Tauga Error4 (uncertainty is 0.01 in surface albedo)	unitless
cldtaua_toterror	Average Cloud Tau Total Uncertainty	unitless
qc_cldtaua_toterror	Quality check results on field: Average Cloud Tau Total Uncertainty	Unitless
reff_i_error1	Effective Radiusi Error1 (1% uncertainty in total irradiance)	unitless
qc_reff_i_error1	Quality check results on field: Effective Radius Error (1% uncertainty in total irradiance)	unitless
reff_i_error2	Effective Radiusi Error2 (uncertainty is standard deviation of calibrated 10 Inought points)	microns
qc_reff_i_error2	Quality check results on field: Effective Radiusi Error2 (uncertainty is standard deviation of calibrated 10 Inought points)	unitless

Variable Name	Long Name	Units
reff_i_error3	Effective Radius Error3 (uncertainty in liquid water path (lwp) 0.001mm larger, using scaling factor with 0.015 mm)	microns
qc_reff_i_error3	Quality check results on field: Effective Radius Error3 (uncertainty in liquid water path (lwp) 0.001mm larger, using scaling factor with 0.015 mm)	unitless
reff_i_error4	Effective Radius Error4 (uncertainty is 0.01 in surface albedo)	microns
qc_reff_i_error4	Quality check results on field: Effective Radius Error4 (uncertainty is 0.01 in surface albedo)	unitless
reff_i_toterror	Instantaneous Effective Radius Total Error	microns
qc_reff_i_toterror	Quality check results on field: Instantaneous Effective Radius Total Error	unitless
reff_a_error1	Effective Radius Error1 (1% uncertainty in total irradiance)	microns
qc_reff_a_error1	Quality check results on field: Effective Radius Error1 (1% uncertainty in total irradiance)	unitless
reff_a_error2	Effective Radius Error2 (uncertainty is standard deviation of calibrated 10 Inought points)	microns
qc_reff_a_error2	Quality check results on field: Effective Radius Error2 (uncertainty is standard deviation of calibrated 10 Inought points)	unitless
reff_a_error3	Effective Radius Error3 (uncertainty in liquid water path (lwp) 0.001mm larger, using scaling factor with 0.015 mm)	microns
qc_reff_a_error3	Quality check results on field: Effective Radius Error3 (uncertainty in liquid water path (lwp) 0.001mm larger, using scaling factor with 0.015 mm)	unitless
reff_a_error4	Effective Radius Error4 (uncertainty is 0.01 in surface albedo)	microns
qc_reff_a_error4	Quality check results on field: Effective Radius Error4 (uncertainty is 0.01 in surface albedo)	unitless
reff_a_toterror	Average Effective Radius Total Error	microns
qc_reff_a_toterror	Quality check results on field: Average Effective Radius Total Error	unitless
cosine_solar_zenith_angle	Cosine Solar Zenith Angle	unitless
qc_cosine_solar_zenith_angle	Quality check results on field: Cosine Solar Zenith Angle	unitless
total_transmittance_filter1	Total transmittance of Narrowband Hemispheric Irradiance, Filter 1	unitless
qc_total_transmittance_filter1	Quality check results on field: Total transmittance of Narrowband Hemispheric Irradiance, Filter 1	unitless
total_transmittance_filter2	Total transmittance of Narrowband Hemispheric Irradiance, Filter 2	unitless

Variable Name	Long Name	Units
qc_total_transmittance_filter2	Quality check results on field: Total transmittance of Narrowband Hemispheric Irradiance, Filter 2	unitless
total_transmittance_filter3	Total transmittance of Narrowband Hemispheric Irradiance, Filter 3	unitless
qc_total_transmittance_filter3	Quality check results on field: Total transmittance of Narrowband Hemispheric Irradiance, Filter 3	unitless
total_transmittance_filter4	Total transmittance of Narrowband Hemispheric Irradiance, Filter 4	unitless
qc_total_transmittance_filter4	Quality check results on field: Total transmittance of Narrowband Hemispheric Irradiance, Filter 4	unitless
total_transmittance_filter5	Total transmittance of Narrowband Hemispheric Irradiance, Filter 5	unitless
qc_total_transmittance_filter5	Quality check results on field: Total transmittance of Narrowband Hemispheric Irradiance, Filter 5	unitless
direct_transmittance_filter1	Direct transmittance of Narrowband Direct Normal Irradiance, Filter 1	unitless
qc_direct_transmittance_filter1	Quality check results on field: Direct transmittance of Narrowband Direct Normal Irradiance, Filter 1	unitless
direct_transmittance_filter2	Direct transmittance of Narrowband Direct Normal Irradiance, Filter 2	unitless
qc_direct_transmittance_filter2	Quality check results on field: Direct transmittance of Narrowband Direct Normal Irradiance, Filter 2	unitless
direct_transmittance_filter3	Direct transmittance of Narrowband Direct Normal Irradiance, Filter 3	unitless
qc_direct_transmittance_filter3	Quality check results on field: Direct transmittance of Narrowband Direct Normal Irradiance, Filter 3	unitless
direct_transmittance_filter4	Direct transmittance of Narrowband Direct Normal Irradiance, Filter 4	unitless
qc_direct_transmittance_filter4	Quality check results on field: Direct transmittance of Narrowband Direct Normal Irradiance, Filter 4	unitless
direct_transmittance_filter5	Direct transmittance of Narrowband Direct Normal Irradiance, Filter 5	unitless
qc_direct_transmittance_filter5	Quality check results on field: Direct transmittance of Narrowband Direct Normal Irradiance, Filter 5	unitless
pwv	Total water vapor along MWR LOS path	cm
qc_pwv	Quality check results on field: Total water vapor along MWR LOS path	unitless
Lwp	Total liquid water along LOS path, it could come from either MWR or the MFRSR with an assumed effective radius	mm

Variable Name	Long Name	Units
qc_lwp	Quality check results on field: Total liquid water along LOS path, it could come from either MWR or the MFRSR with an assumed effective radius	unitless
ir_temp	IR Brightness Temperature	K
qc_ir_temp	Quality check results on field: IR Brightness Temperature	unitless
Cloudfraction	Estimated Average Fractional Sky Cover over the Hemispheric Dome (cf)	unitless
qc_cloudfraction	Quality check results on field: Estimated Average Fractional Sky Cover over the Hemispheric Dome (cf)	unitless
cloudbasebestestimate	LASER Cloud Base Height Best Estimate	m AGL
qc_cloudbasebestestimate	Quality check results on field: LASER Cloud Base Height Best Estimate	unitless
lwp_uncertainty	Lwp uncertainty if derived from mfrsr.b1	mm
qc_lwp_uncertainty	Quality check results on field: lwp uncertainty if derived from mfrsr.b1	unitless
lwp_source	Flag indicating data source used to determine lwp	unitless
surface_albedo	Surface Albedo	unitless
qc_surface_albedo	Quality check results on field: Surface Albedo	unitless
Io_time	Langley time series	Day fraction offset from 00:00 on this day
Io_filter1	Solar constant corrected for solar distance for the Direct Narrowband Filter1	counts
qc_Io_filter1	Quality check results on field: solar constant corrected for solar distance for the Direct Narrowband Filter1	unitless
Io_filter2	Solar constant corrected for solar distance for the Direct Narrowband Filter2	counts
qc_Io_filter2	Quality check results on field: solar constant corrected for solar distance for the Direct Narrowband Filter2	unitless
Io_filter3	Solar constant corrected for solar distance for the Direct Narrowband Filter3	counts
qc_Io_filter3	Quality check results on field: solar constant corrected for solar distance for the Direct Narrowband Filter3	unitless
Io_filter4	Solar constant corrected for solar distance for the Direct Narrowband Filter4	counts
qc_Io_filter4	Quality check results on field: solar constant corrected for solar distance for the Direct Narrowband Filter4	unitless

Variable Name	Long Name	Units
Io_filter5	Solar constant corrected for solar distance for the Direct Narrowband Filter5	counts
qc_Io_filter5	Quality check results on field: solar constant corrected for solar distance for the Direct Narrowband Filter5	unitless
Io_flag_filter1	Inought flag rejection flag for Direct Narrowband Filter1	unitless
Io_filter1_final	The final Inought that is used to determine total transmission	W/(m <sup>2</sup> nm)
cal_start_date	Start day for the Io data selected for calibration	Day fraction offset from 00:00 on this day
cal_end_date	End day for the Io data selected for calibration	Day fraction offset from 00:00 on this day
Io_filter1_standard_deviation	Standard deviation of Inought to the closest 10 points around the run day	W/(m <sup>2</sup> nm)
lat	North latitude	degree_N
lon	East longitude	degree_E
alt	Atitude above mean sea level	



[www.arm.gov](http://www.arm.gov)

U.S. DEPARTMENT OF  
**ENERGY**

---

Office of Science